

PAMELA silicon tracking system: Experience and operation

S. Ricciarini

INFN, Structure of Florence, Florence, Italy

On behalf of the PAMELA collaboration

Available online 1 August 2007

Abstract

The PAMELA cosmic-ray telescope has been launched into space on 15 June 2006 on board of the Resurs-DK1 Russian satellite and is in continuous data acquisition mode since 11 July 2006. The magnetic spectrometer of PAMELA is composed of a hollow permanent magnet with a microstrip Si tracking system inserted inside the cavity. This paper reviews the general characteristics of the tracking system and presents a preliminary analysis of a data sample acquired in flight, showing that the main performances of the Si detectors after launch are in agreement with what expected on the basis of the ground qualification tests.

© 2007 Elsevier B.V. All rights reserved.

PACS: 95.55.Vj; 95.85.Ry; 95.35.+d

Keywords: PAMELA; Cosmic rays; Silicon tracker; Space experiment

1. Introduction: the PAMELA experiment

PAMELA [1] (a Payload for Antimatter Matter Exploration and Light-nuclei Astrophysics) is a satellite-borne experiment designed to study charged particles in the cosmic radiation, focusing on antiparticles (antiprotons and positrons).

The main scientific objective is the precise measurement of the energy spectra for antiprotons \bar{p} (range 80 MeV–190 GeV) and positrons e^+ (50 MeV–270 GeV) in cosmic rays, together with e^- , p, light nuclei and their isotopes, in order to search for evidence of dark-matter particles annihilations, to test cosmic-ray propagation models and to search for direct evidence of antinuclei (in particular $\overline{\text{He}}$, with a sensitivity in the $\overline{\text{He}}/\text{He}$ ratio of $\sim 10^{-7}$).

The PAMELA cosmic-ray telescope (Fig. 1) is housed in a pressurized Al vessel, filled with N_2 at 1 atm, on-board of the Resurs-DK1 satellite, which follows a semi-polar orbit with altitude varying between 350 and 600 km and inclination of 70° . PAMELA is in continuous data acquisition mode since 11 July 2006; the mission is foreseen to last at least 3 years.

The telescope has maximum diameter 102 cm and height 130 cm; its mass is 470 kg and the maximum power consumption is 355 W. PAMELA is composed of several specialized detectors.

- The core of the instrument is a magnetic spectrometer with Si tracking system (see Section 2) to determine the particle charge sign and momentum through the trajectory reconstruction in the magnetic field.
- A time-of-flight system (TOF, ~ 250 ps resolution for p/\bar{p} and e^\pm) with three double planes (S1, S2, S3) of fast plastic scintillator, gives the main trigger signal, rejects upward going particles (albedo) and measures the particle velocity, which is used for identification at kinetic energies below ~ 1 GeV. The absolute value of the charge is given by the ionization measurement in the TOF scintillators and in the Si layers of the tracking system.
- A W/Si sampling electromagnetic calorimeter [2], with total depth of 16.3 radiation lengths and 0.6 nuclear interaction lengths, discriminates between leptons and hadrons (e.g. e^+ from the background of p) for kinetic energies above ~ 1 GeV, with contaminations $\sim 10^{-4}$ or better and detection efficiencies of $\approx 90\%$. The calorimeter also directly measures the e^\pm energy, with

E-mail address: ricciarini@fi.infn.it

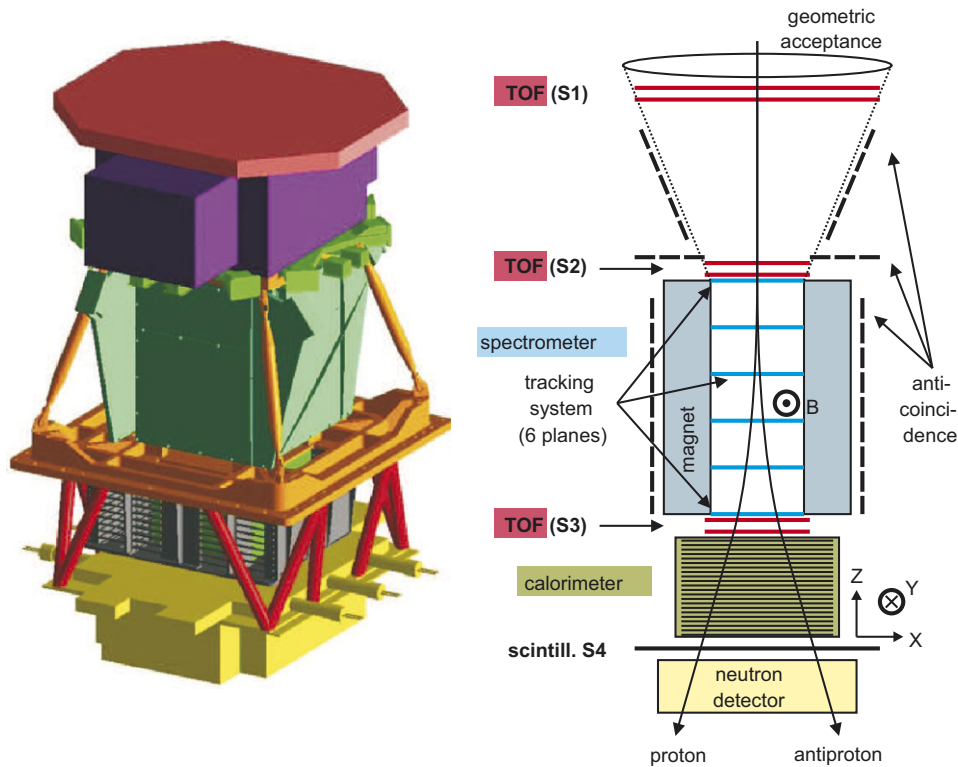


Fig. 1. Three-dimensional view and section of the PAMELA cosmic-ray telescope, with illustrated the principle of discrimination between particle and antiparticle in the magnetic spectrometer. The PAMELA reference system and the main direction of magnetic field inside the cavity of the spectrometer are also shown.

resolution $\approx 5.5\%$ at energies above 20 GeV and up to at least 200 GeV.

- An anticoincidence system (scintillator planes) detects particles entering the apparatus from outside the acceptance.
- A neutron detector (polyethylene moderator and ^3He proportional counters) and a further scintillator plane (S4) complement the calorimeter in the lepton/hadron discrimination.

2. The magnetic spectrometer and the Si tracking system

The magnetic spectrometer [3], designed and developed by the Florence group of the PAMELA collaboration, is conceived to give a precise measurement of momentum modulus and charge (with sign) of the incident particle, at the same time satisfying the strong limits, imposed by the satellite mission, in available mass, volume, power and data bandwidth for transmission to ground. A compact mechanical assembly has been chosen and tested to withstand the stresses during the launch phase. All the electronic components have been space qualified by means of radiation-hardness tests, taking into account the expected particle fluxes over the 3-year duration of the mission.

The spectrometer is composed of a permanent magnet, with an internal rectangular cavity, and a tracking system with six planes of double-sided Si microstrip detectors,

uniformly positioned along the cavity. Each plane independently measures both the X and Y coordinates of the crossing point of an incoming ionizing particle.

The magnet is a tower 43.66 cm high, formed by five superposed identical modules with a central rectangular cavity (16.14 cm \times 13.14 cm), with a total geometric factor of 21.6 cm² sr. Each module is composed of 12 Nd-Fe-B alloy elements with high residual magnetic induction (≈ 1.32 T), in such a way that the field inside the cavity is quasi-dipolar, with practically all the strength along the Y axis and with a good uniformity.¹

2.1. Silicon tracking system

The tracking system is composed of six planes of high-precision Si microstrip detectors, positioned between the five magnetic modules and on top and bottom of the magnetic tower, with uniform vertical spacing of 8.9 cm. Each plane (see Fig. 2) is divided into three independent sections (*ladders*) along the X axis and housed in an Al support frame. A *ladder* is formed by two rectangular (5.33 cm \times 7.00 cm \times 300 μm) double-sided n-type Si sensors (produced by Hamamatsu [4]) and a hybrid circuit, with Al₂O₃ substrate, containing the front-end electronics.

¹The intensity of X and Z field components are less than 10% of Y component, whose average value is 0.43 T; variations of field intensity are $<10\%$ over 80% of the cavity volume.

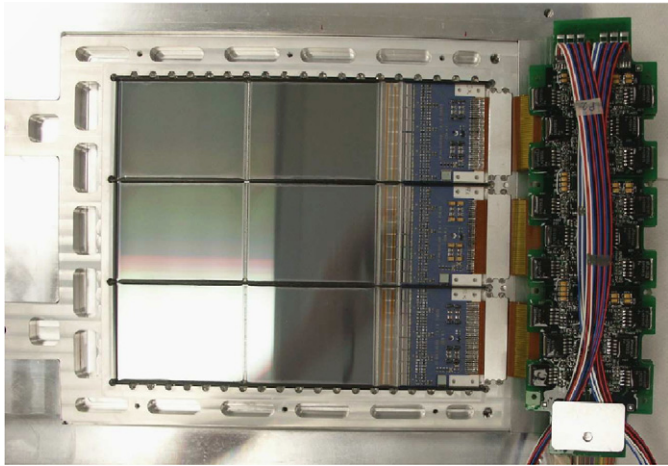


Fig. 2. One plane of the tracking system, completed with the ADC electronics on separate boards (on the right). On the same edge of the plane are the three hybrid circuits, corresponding to the three independent ladders.

The strip implant pitch on the sensors is $25.5\ \mu\text{m}$ for the junction side ($2035\ \text{p}^+$ strips) and $66.5\ \mu\text{m}$ for the ohmic side ($1024\ \text{n}^+$ strips); strips on opposite sides are orthogonal. The junction side (or X view) is used to measure the impact-point X coordinate in the main bending plane XZ , orthogonal to the magnetic field. The charge read-out is performed for one out of two strips on the X view and for all the strips on the ohmic (Y) view, through an integrated capacitive coupling of $\approx 20\ \text{pF}/\text{cm}$, obtained by means of a thin ($0.1\ \mu\text{m}$) insulating layer of SiO_2 between implant strip and superposed read-out electrode.

A reverse-bias voltage of $+80\ \text{V}$ is applied between ohmic-side and junction-side strips to completely deplete the substrate; the bias is fed through a guard ring surrounding the strips. To avoid applying the bias across the SiO_2 read-out capacities, the reference (“ground”) voltages of the front-end electronics are short-circuited with the voltages applied to the strips of the corresponding side; therefore the reference voltage for the Y -view electronics is $+80\ \text{V}$ above the one for the X view, which coincides with the ground of the PAMELA apparatus. Inductive decoupler chips (ADuM1100 [6]) are present on the digital lines between the ADC stage and the following stage (DSP boards, see below).

On the X view of the ladder the corresponding electrodes of the two sensors are soldered together through wire bonds ($17\ \mu\text{m}$ diameter), for a total of 1018 read-out channels. On the Y view a second level of 1024 metallic tracks, orthogonal to the first level of read-out electrodes, brings the signals toward the same edge of the ladder as for the X view, where the hybrid circuit is placed. With this arrangement each Y channel is associated with two different read-out electrodes, one per sensor and $7\ \text{cm}$ apart; the ambiguity thus introduced can be easily solved with the position information from other detectors.

The front-end electronics for each side of a ladder is formed by 8 VA1 [5] chips housed on the corresponding

side of the hybrid circuit. The VA1 contains 128 low-noise and low-power independent acquisition chains (charge preamplifier, CR-RC shaper, track-and-hold) and a multiplexer/shift-register for sequential read-out. The operating point has been chosen as optimal compromise between power consumption and voltage gain: the former is set to $1.0\ \text{mW}/\text{channel}$, giving $37\ \text{W}$ total dissipation for the 288 VA1 of the tracking system; the latter is set to $7.0\ \text{mV}/\text{fC}$ thus having VA1 output saturation at ~ 10 MIP signal.

The second-stage (ADC) electronics is housed on printed-circuit boards positioned in the vicinity of the planes; for each side of a ladder there is a dedicated board section with a 12-bit ADC (AD7476A [6]) and control logics on an FPGA chip (A54SX16P [7]), connected with the corresponding hybrid through a $5\ \text{cm}$ long flat kapton cable.

The 36 ADC sections are operated in parallel at $0.5\ \text{MSPs}$, for a total event acquisition time of $2.1\ \text{ms}$. The digitized data are compressed on DSP boards, equipped with Digital Signal Processors ADSP2187L [6] (one per view); the typical compression time is $1.1\ \text{ms}$ and the compression factor is 15, thus producing a total of $\approx 4\ \text{kbyte}/\text{event}$.

2.2. Expected spatial, momentum and charge resolution

The spatial resolution of the Si detectors is determined by the channel pitch and the cluster signal/noise²; the best performance is obtained using the non-linear η algorithm for reconstruction of the impact point [10]. The spatial resolution has been studied with several beam tests; typical values for normally incident particles are $3.0\ \mu\text{m}$ (X view) and $11.5\ \mu\text{m}$ (Y view).

With the last beam test of PAMELA flight model (CERN SPS, 2003) the overall performances of the spectrometer have been determined and the Si sensors have been aligned with protons of known momentum. The alignment has been checked and completed with cosmic rays (with incidence angles distributed over the whole geometric acceptance) collected at ground level during the final qualification tests of PAMELA at Rome “Tor Vergata” INFN laboratories (2005). The alignment parameters after launch will be monitored with high-energy electrons after collecting enough statistics.

The momentum resolution of the spectrometer critically depends on the spatial resolution of the X (bending) view. Measurements performed at the CERN SPS 2003 beam test with protons of known momentum gave a maximum detectable rigidity³ of $\approx 1\ \text{TV}$ (Fig. 3).

The particle charge discrimination capability of the tracking system has been studied with a dedicated beam

²See Section 3.3 for definitions.

³Defined as the absolute value of rigidity for which the relative uncertainty of the measurement is equal to 1. The rigidity R is defined as the ratio between momentum modulus P and charge Q of the particle: $R = P \cdot c/Q$.

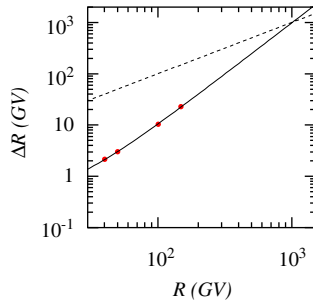


Fig. 3. Uncertainty in rigidity measurement, obtained with proton beams at CERN SPS. The dashed line is the bisector $\Delta R = R$. The fit to the four experimental points (continuous curve) assumes a contribution from multiple scattering (in the limit $\beta \sim 1$) $\Delta R_{ms} \propto R$ and one from spatial resolution $\Delta R_{sr} \propto R^2$. The intersection of the two curves gives the maximum detectable rigidity of the spectrometer.

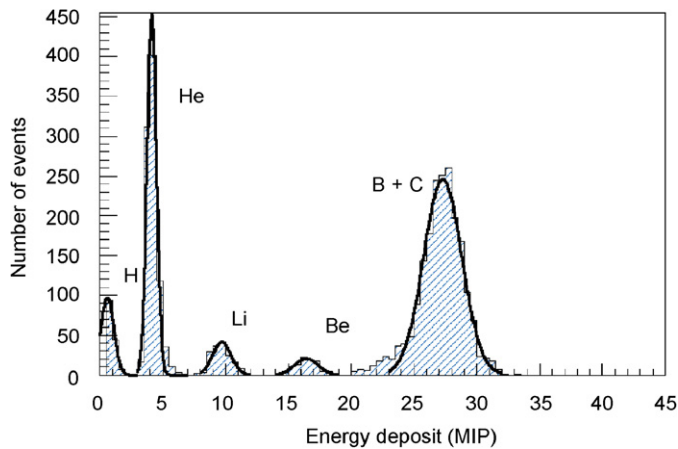


Fig. 4. Energy deposit per cluster (averaged on different Si detector planes) for products of fragmentation of ^{12}C on various targets at GSI beam test.

test at GSI [8] in 2006 using a spare set of Si detector planes. Results [9], shown in Fig. 4, indicate that nuclei up to $Z = 4$ can be clearly identified; on the other hand, the single-channel saturation at ~ 10 MIP affects the charge discrimination capability for higher- Z nuclei.

3. Performances of the tracking system after launch

A first evaluation of the actual performances of the tracking system Si detectors after launch has been done through a preliminary analysis of a sample of data taken during ~ 12 h of flight. Data show that the tracking system is working nominally as expected.

3.1. Thermal environment

A stable thermal environment is fundamental to guarantee stability of operation for the various mechanical and electronic components of the magnetic spectrometer.

The main source of heat is the VA1 chips on the Al_2O_3 hybrid circuits of the detector planes, compactly assembled

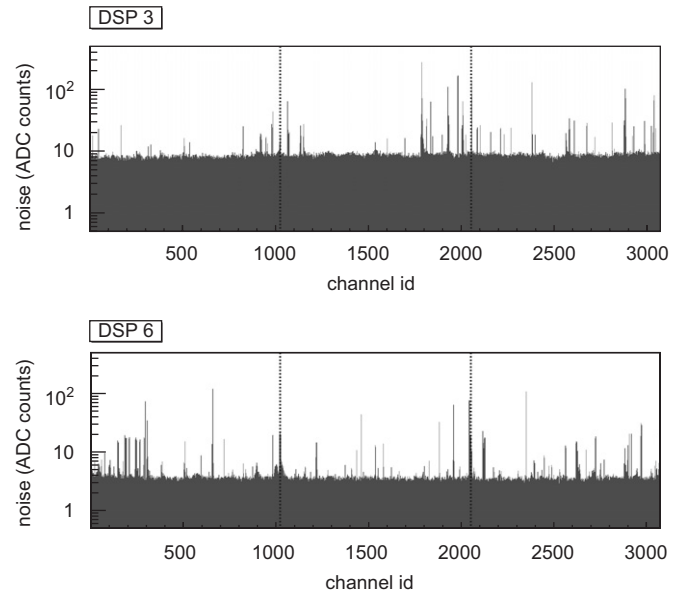


Fig. 5. Flight data: noise profiles for a Y view (DSP 3) and an X view (DSP 6). Note the three independent ladders (1024 channels each).

within the magnetic tower: for the internal planes the double-sided hybrid circuit is positioned between two superposed magnetic modules, with a gap of less than 4 mm on each side. Convection heat transfer in the PAMELA pressurized container filled with N_2 is negligible because of the low gravity; heat flows mainly through radiation toward the nearby magnetic modules⁴ and is then transferred to the PAMELA cooling loop pipe (with liquid pumped by the satellite), directly connected to the external walls of all the five modules, where thermal sensors (AD590 [6]) are placed.

Data collected through these sensors show that the cooling system is working efficiently:

- with all PAMELA systems powered-off the typical module temperature is $\approx 21^\circ\text{C}$, with variations of $< 1^\circ\text{C}$ between different modules; after power-on, temperature increases in a few hours to a steady value of less than 31°C ;
- temperatures remain very stable ($< 1^\circ\text{C}$ variations) along the orbit, despite the different sun lighting conditions. The orbit duration is about 94 min.

3.2. Electronic noise

Fig. 5 shows typical noise profiles taken in flight for an X and a Y view (after common-mode noise subtraction). Similar profiles for the 12 views are obtained at each on-line calibration of the tracking system, which is done about once per orbit.

Typical noise values for good channels are ≈ 510 ENC for X views and ≈ 1090 ENC for Y views; these values do

⁴The internal walls of the modules are coated with IR absorbing paint (Nextel Velvet Coating 811-21 with Verdunner 8061).

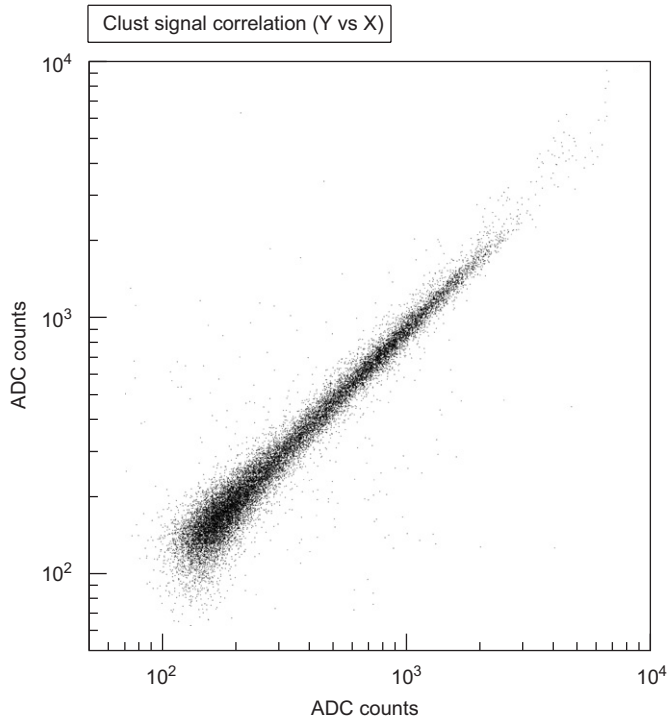


Fig. 6. Flight data: Y – X cluster signal correlation for one plane.

not show significant variations with time. The X – Y difference is related to the channel capacitance to ground, <10 pF for the X (junction) view, <20 pF for the Y (ohmic) view because of the double metal layer.

Bad channels are identified with the on-line calibration in the low- and high-noise tails of the noise profile for each VA1 chip (128 channels); during subsequent physics runs these channels are excluded from computation of event common-mode noise, but they are still read-out together with good channels. The fraction of bad channels for a view ranges from 4% to 5%; no significant variation in the number of bad channels has been observed after the launch.

Bad channels originate from defects on the Si sensors (broken read-out capacitances, short-circuits between adjacent channels or interrupted channels), defects in the wire bondings between the two sensors and the hybrid, failures of VA1 chips read-out channels. Defects on sensors range between 0.39% and 1.81%, with an average value of 1.05%.

3.3. Particle detection performances

A sample of events with “clean” single tracks has been selected to study the particle detection performances of the

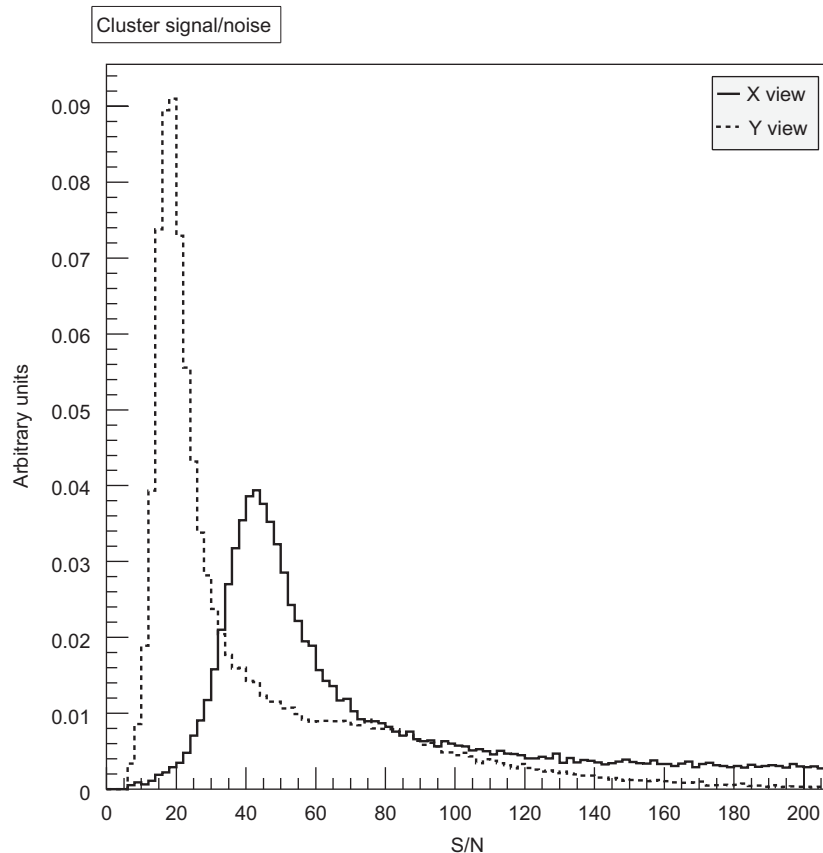


Fig. 7. Flight data: distribution of cluster signal/noise ratio for one plane.

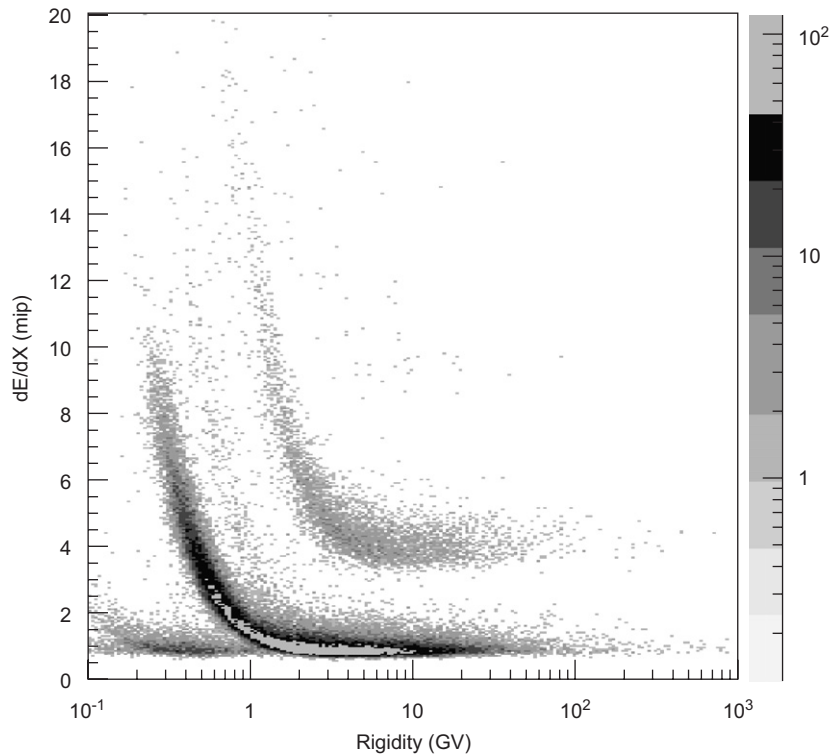


Fig. 8. Flight data: distribution of average released energy versus particle rigidity.

Si sensors. Note that this sample contains both MIP and non-MIP particles, incident on the detectors with angles respect to the Z axis up to $\approx 20^\circ$ in the XZ plane and up to $\approx 16^\circ$ in the YZ plane (the inclination is limited by the geometric acceptance of the spectrometer).

A *cluster seed* is identified on a *ladder* when the channel signal/noise ratio (S/N) is above a fixed threshold (set to 7 for this analysis); channels adjacent to the *seed* on both sides are included in the cluster if their S/N exceeds a lower threshold (set to 4).

Typical cluster multiplicities for normally incident MIP are two channels (X view) and one channel (Y view).

The *cluster signal* is defined as the sum of the signals over all channels included in the cluster. Fig. 6 shows the cluster signal correlation between X and Y view for one plane.

The *cluster S/N* is defined as the sum of the S/N over all the cluster channels. The distribution of the cluster S/N for the same plane as above is in Fig. 7. Average cluster S/N for the MIP subsample are consistent with those measured at beam-tests: ≈ 56 (X view) and ≈ 26 (Y view), with variations between different planes up to 10%.

Fig. 8 shows a preliminary plot of the energy dE/dX released by the incident particle (averaged over the various planes) as a function of the measured rigidity. The most abundant elements (H, He) are clearly identified; also d/p discrimination is quite good.

References

- [1] P. Picozza, A.M. Galper, G. Castellini, et al., *Astropart. Phys.* 27, 4 (2007) 296; M. Boezio et al., in: *Proceedings of the 29th ICRC, Pune, vol. 10, 2005*, p. 255; (<http://wizard.roma2.infn.it/pamela>).
- [2] M. Boezio, et al., *Nucl. Instr. and Meth. A* 487 (2002) 407.
- [3] O. Adriani, et al., *Nucl. Instr. and Meth. A* 511 (2003) 72; L. Bonechi, et al., *Nucl. Phys. B (Proc. Suppl.)* 125 (2003) 308; F. Taccetti, et al., *Nucl. Instr. and Meth. A* 485 (2002) 78; (<http://hep.fi.infn.it/PAMELA>).
- [4] (<http://sales.hamamatsu.com>).
- [5] (<http://www.ideas.no>).
- [6] (<http://www.analog.com>).
- [7] (<http://www.actel.com>).
- [8] (<http://www.gsi.de>).
- [9] R. Sparvoli et al., in: *Proceedings of the 20th ECRS, Lisbon, 2006*.
- [10] S. Straulino, et al., *Nucl. Instr. and Meth. A* 556 (2006) 100.